



# Light-Driven Reduction of CO<sub>2</sub> to CO by Cobalt (II) bis-(pyrazolyl)phenantroline Complexes

Jorge Ferreira Jr, Gabriela Uez, Angélica V. Moro, Diogo S. Ludtke, Adriana C. A. Casagrande, Pedro Migowski, Fabiano S. Rodembusch, Osvaldo L. Casagrande Jr, \*

<sup>1</sup> Laboratory of Molecular Catalysis, Instituto de Química, Universidade Federal do Rio Grande do Sul, Avenida Bento Gonçalves, 9500, 90501-970, Porto Alegre, RS (Brazil).

#### Resumo/Abstract

# **RESUMO**

A síntese, caracterização e avaliação fotocatalítica de complexos de cobalto(II) bis(pirazolil)fenantrolina (Co1–Co3) para a redução de CO<sub>2</sub> a CO são descritas. Os complexos foram totalmente caracterizados, e a estrutura do Co2 foi confirmada por difração de raios X. As reações fotocatalíticas utilizando [Ru(bipy)<sub>3</sub>]<sup>2+</sup> como fotosensibilizador e BIH como doador sacrificial mostraram que o Co2, contendo grupos doadores de elétrons (metila), apresentou a maior atividade e seletividade, alcançando um TON<sub>CO</sub> de 896 e seletividade para a produção de CO (82%) após 24 h. Estudos sistemáticos demonstraram que a diminuição da concentração do catalisador aumenta significativamente a atividade catalítica e a seletividade para CO, atingindo TON<sub>CO</sub> de até 11.753 e seletividade superior a 94%. O tempo maior de irradiação levou a um aumento na produção de CO, embora com eficiência significativamente reduzida após 24 horas. Esses resultados destacam o potencial de complexos de cobalto como catalisadores homogêneos eficientes e seletivos para a fotorredução de CO<sub>2</sub> em condições brandas.

Palavras-chave: Redução de CO<sub>2</sub>, fotocatálise, complexos de cobalto(II), ligantes nitrogenados tetradentados

### ABSTRACT -

The synthesis, characterization, and photocatalytic evaluation of cobalt(II) bis(pyrazolyl)phenanthroline complexes ( $Co_1$ – $Co_3$ ) for the visible-light-driven reduction of  $CO_2$  to CO are discribed. The complexes were fully characterized, and the structure of  $Co_2$  was confirmed by X-ray crystallography. Photocatalytic experiments using  $[Ru(bipy)_3]^{2+}$  as photosensitizer and BIH as sacrificial donor revealed that  $Co_2$ , bearing electron-donating methyl groups, exhibited the highest activity and selectivity, reaching a  $TON_{CO}$  of 896 and 82% CO selectivity after 24 h. Systematic studies demonstrated that lowering catalyst concentration significantly enhances TON and CO selectivity, achieving  $TON_{CO}$  up to 11,753 and selectivity above 94%. Prolonging the irradiation time led to increased CO production, albeit with markedly reduced efficiency beyond 24 hours. These results highlight the potential of cobalt complexes with tailored electronic environments as efficient and selective homogeneous catalysts for  $CO_2$  photoreduction under mild conditions.

Keywords: CO2 reduction, photocatalysis, cobalt (II) complexes, nitrogen tetradentate ligands

# 1. Introduction

The escalating atmospheric concentration of carbon dioxide (CO<sub>2</sub>), primarily resulting from the combustion of fossil fuels and industrial activities, poses a significant environmental challenge in the context of global climate change. As the predominant anthropogenic greenhouse gas, CO<sub>2</sub> contributes substantially to global warming. Mitigating this issue necessitates not only efficient strategies for carbon capture and storage (CCS) but also the development of sustainable methodologies for the transformation of CO<sub>2</sub> a thermodynamically stable and kinetically inert molecule

into value-added chemicals and fuels.(1-3) A broad spectrum of  $\mathrm{CO}_2$  capture technologies has been extensively investigated, including chemical absorption, physisorption using porous solid sorbents, and membrane-based separations. While these approaches are effective in reducing  $\mathrm{CO}_2$  emissions at the point of source, they do not inherently address the persistent accumulation of  $\mathrm{CO}_2$  in the atmosphere. In this regard, the catalytic conversion of  $\mathrm{CO}_2$  into industrially relevant chemicals such as carbon monoxide ( $\mathrm{CO}$ ), formic acid, and methane has emerged as a promising route for carbon valorization.(4-5) Among the possible products, the selective two-electron reduction of



CO<sub>2</sub> to CO is particularly attractive due to the utility of CO as a key intermediate in several industrial processes, including the Fischer–Tropsch synthesis and the production of synthetic fuels.(6-7) Within the broader domain of CO<sub>2</sub> utilization, the photocatalytic reduction of CO<sub>2</sub> using homogeneous catalysts has gained increasing attention, driven by the prospect of coupling this transformation with solar energy harvesting a renewable and sustainable energy source.(8-10)

The photocatalytic conversion of CO<sub>2</sub> to CO involves multielectron and multiproton transfer steps, often under thermodynamically uphill conditions, making catalyst design a critical parameter for achieving high efficiency, selectivity, and stability. Homogeneous photocatalysts offer several advantages in this context, including well-defined coordination environments, tunable redox properties, and the ability to operate under mild conditions with minimal formation of undesired byproducts. Transition-metal-based homogeneous catalysts particularly those incorporating ruthenium, rhodium, and iridium complexes have demonstrated notable performance in terms of activity and selectivity. However, the high cost, scarcity, and sustainability concerns associated with these noble metals pose significant limitations for their large-scale deployment.

Consequently, current research efforts have increasingly focused on the development of catalysts based on earthabundant first-row transition metals which offer compelling advantages, including low toxicity, high natural abundance, and redox potentials amenable to ligand modulation, thereby enabling the rational design of cost-effective and environmentally benign photocatalytic systems. Among them, cobalt complexes (11-15) have emerged as state-ofthe-art homogeneous photocatalysts for CO2-to-CO conversion, owing to their favorable redox properties, tunable coordination environments, and demonstrated efficiency under visible-light irradiation. In this work, we report on recent progress in the development of homogeneous cobalt(II) catalysts coordinated with nitrogen-based ligands for the photocatalytic reduction of CO<sub>2</sub> to CO. Our study focuses on elucidating key structureactivity relationships governing catalytic performance, particularly in terms of efficiency, product selectivity, and operational stability under visible-light irradiation."

# 2. Experimental

#### 3.1 Materials

All solvents used in the synthesis of catalysts and photocatalytic reactions were dried over a MBraun SPS-800 solvent purification system. Co(ClO<sub>4</sub>)<sub>2</sub>·6H<sub>2</sub>O and [Ru(bipy)<sub>3</sub>]Cl<sub>2</sub> were purchased from Sigma-Aldrich and used as received. BIH (1,3-dimethyl-2-phenyl-2,3-dihydro-1H-benzo[d]-imidazole) was prepared according to the reported procedure.(16) The tetradentate nitrogen ligands such as 2,9 bis-(pyrazol-1-yl)-1,10-phenanthroline



(**bpzphen**), 2,9 bis-(3,5-dimethyl-1H-pyrazol-1-yl)-1,10phenanthroline (bpzMe2phen) e 2,9 bis-(3-diphenyl-1Hpyrazol-1-yl)-1,10-phenanthroline (bpz<sup>Ph</sup>phen) prepared as described in the literature.(17) Infrared spectra were performed on neat products using a FT-IR Bruker Alpha Spectrometer operating in the ATR mode. <sup>1</sup>H and <sup>13</sup>C NMR chemical shifts are reported in ppm vs. SiMe<sub>4</sub> and were determined by reference to the residual solvent peaks. Elemental analyses were performed by the Analytical Central Service of the Institute of Chemistry-UFRGS (Brazil) and are the average of two independent determinations. High-resolution mass spectrometry (HRMS) data were collected on a Micromass Waters® Q-Tof spectrometer.

#### 3.2 Synthesis of cobalt complexes

3.2.1 [Co(bpzphen)( $H_2O$ )<sub>2</sub>]( $ClO_4$ )<sub>2</sub> ( $Col_1$ ). A solution of  $Co(ClO_4)_2$ · $6H_2O$  (0.1094 g, 0.32 mmol) in acetonitrile (10 mL) was added into a solution of dpzphen (0.1000 g, 0.32 mmol) in acetonitrile (8 mL). The resulting mixture was stirred at 25°C for 24 hours. The reaction volume was concentrated (3 mL) and diethyl ether (15mL) was added generating a pink solid. The solid residue was washed repeatedly with diethyl ether (3 ×10 mL) to give, after drying,  $Col_1$  as a pale pink solid. (0.1649 g, 85% yield). Anal. Calc. for  $Cl_1$ H<sub>16</sub>Cl<sub>2</sub>CoN<sub>6</sub>O<sub>10</sub>: C: 35.66, H: 2.66, N: 13.86. Found: C: 35.70, H: 2.72, N: 13.47. ESI-HRMS (CH<sub>3</sub>OH, m/z) Anal. Calcd. for  $Cl_1$ H<sub>12</sub>CoN<sub>6</sub>: 185.5227. Found: 185.5222 [Co(bpzphen)]<sup>+2</sup>.

3.2.2 [Co(bpz<sup>Me2</sup>phen)(H<sub>2</sub>O)<sub>2</sub>](ClO<sub>4</sub>)<sub>2</sub> (**Co2**). This complex was prepared as described above for **Co1**, starting from dpz<sup>Me2</sup>phen (0.1000 g, 0.27 mmol) and Co(ClO<sub>4</sub>)<sub>2</sub>·6H<sub>2</sub>O (0.09879 g, 0.27 mmol) in acetonitrile (20 mL) to give **Co2** as pale brown solid (0.1573 g, 88% yield). Anal. Calc. for C<sub>22</sub>H<sub>24</sub>Cl<sub>2</sub>CoN<sub>6</sub>O<sub>10</sub>: C: 39.90, H: 3.65, N: 12.69. found: C: 39.78, H: 3.56, N: 12.11. ESI-HRMS (CH<sub>3</sub>OH, m/z) Anal. Calcd. for C<sub>22</sub>H<sub>20</sub>CoN<sub>6</sub>: 213.5540. Found: 213.5535 [Co(dpz<sup>Me2</sup>phen)]<sup>+2</sup>.

 $3.2.3 \, [Cobpz^{Ph}phen)(H_2O)_2](ClO_4)_2 \, (\textbf{Co3})$ . This complex was prepared as described above for Co1, starting from dpz<sup>Ph</sup>phen (0.1000 g, 0.21 mmol) and Co(ClO<sub>4</sub>)<sub>2</sub>·6H<sub>2</sub>O (0.07684 g, 0.21 mmol) in acetonitrile (20 mL) to give Co3 as pale brown solid (111 mg, 70% yield). Anal. Calc. for  $C_{30}H_{24}Cl_2CoN_6O_{10}$ : C: 47.51, H: 3.19, N: 11.08. found: C: 47.13, H: 2.95, N: 10.89. ESI-HRMS (CH<sub>3</sub>OH, m/z) Anal. Calcd. for  $C_{30}H_{20}CoN_6$ : 261.5540. Found: 261.5524  $[Co(dpz^{Ph}phen)]^{+2}$ .

#### 3.3 Photocatalytic CO<sub>2</sub> reduction

Photocatalytic  $CO_2$  reduction was performed in a borosilicate photoreactor designed in our group (volume = 12.0 mL) containing a solution of the catalyst (0.05 mM),  $[Ru(bipy)_3]^{2+}$  (0.3 mM) and BIH (0.11 M) in a  $CO_2$ -saturated aqueous  $CH_3CN$  solution (7.5% v/v) (4.0 mL). The photoreactor was sealed with a rubber septum and then purged with  $CO_2$  for 20 mins. The photoreactor was placed

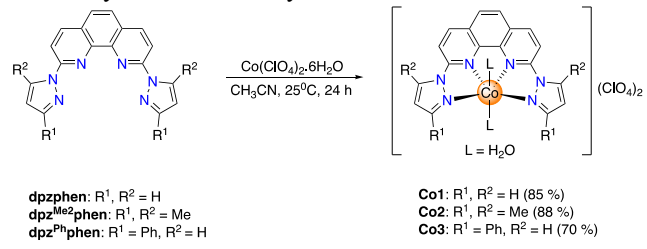


inside the illumination chamber equipped with LED strip (blue light,  $\lambda = 460 \text{ nm}$ ) with light irradiance  $403 \mu\text{Wcm}^{-1}$ <sup>2</sup>nm<sup>-1</sup>(measured using an Ocean Optics). The distance of the reactor external wall to the light source was 5 cm. Quantitative gas chromatographic analysis from the gas evolved in the headspace were performed with an Agilent Technologies 7890A GC system equipped with a thermal conductivity detector in series with a methanizer and FID detector. CO and H<sub>2</sub> production were quantitatively assessed using a Petrocol HD capillary column (methyl silicone, 100 m length, 0.25 mm i.d. and film thickness of 0.5 μm) (36 °C for 15 min, then heating at 5 °C·min-1 until 250 °C). 50 μL of gas phase samples were taken using a 100-uL gastight Hamilton sirynge and injected in the GC in splitless mode. Calibration curves for H2 and CO were determined separately by injecting known quantities of a standard mixture (MULT MIX HC - OX - Air Liquide) containing 1,00000 % mol of hydrogen and 1,00000 % of carbon monoxide.

# 3. Results and Discussion

# 3.1 Synthesis and Characterization of cobalt complexes

The desired tetradentate bis(pyrazolyl)phenanthroline ligands were efficiently synthesized through a nucleophilic aromatic substitution (SNAr) reaction between 2,9-dibromo-1,10-phenanthroline and the corresponding pyrazole derivative. [Error! Bookmark not defined.7] The reaction of bis-(pyrazolyl)phenantroline ligands with 1 equiv of Co(ClO<sub>4</sub>)<sub>2</sub>·6H<sub>2</sub>O in CH<sub>3</sub>CN at 25°C yielded the corresponding cobalt(II) complexes which were isolated in good to excellent yields (70–88%) (Scheme 1). These complexes were characterized by elemental analysis, FTIR spectroscopy, high-resolution mass spectrometry (HRMS) and X-ray diffraction analysis for Co2.



**Scheme 1**. Synthesis of cobalt(II) complexes

The elemental analysis data support the formation of the target compounds of general formula [Co(dpz<sup>R</sup>phen)(H<sub>2</sub>O)<sub>2</sub>](ClO<sub>4</sub>)<sub>2</sub> (R = H, Me, Ph), featuring the coordination of two water molecules, in agreement with previous observations for related cobalt-based analogues.(11-15) Single-crystals of Co2 suitable for X-ray diffraction analysis were obtained from slow diffusion of diethyl ether into a saturated CH<sub>3</sub>CN solution. An ORTEP representation of Co2 is depicted in Figure 1, where the



displacement ellipsoids are drawn at the 50% probability level.

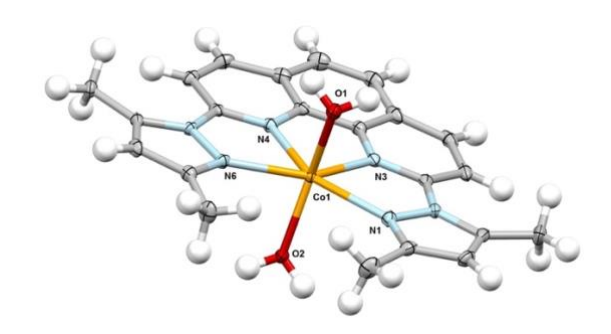


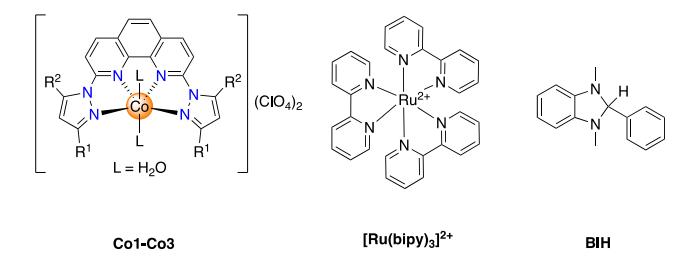
Figure 1. ORTEP view of Co2. Displacement ellipsoids are drawn at the 50% probability level; only one of the two chemically equivalent but crystallographically distinct molecules is shown; The counterions are omitted for clarity. Selected bond distances (Å) and angles (deg): N(1)-Co(1) = 2.215(2), N(3)-Co(1) = 2.100(2), N(4)-Co(1) = 2.095(2), N(6)-Co(1) = 2.2171(16), O(1)-Co(1) = 2.1000(18), O(2)-Co(1) = 2.0443(19), O(2)-Co(1)-N(4) =104.26 (8), O(2)-Co(1)-O(1) = 152.07(7), N(4)-Co(1)-O(1) =97.44(8), O(2)-Co(1)-N(3) = 106.02(8), N(4)-Co(1)-N(3)76.41(8), O(1)-Co(1)-N(3) = 95.93(8), O(2)-Co(1)-N(1)N(4)-Co(1)-N(1) = 147.93(8), O(1)-Co(1)-N(1) =85.48(7), 85.33(7), N(3)-Co(1)-N(1) = 71.53(8), O(2)-Co(1)-N(6)83.87(7), N(4)-Co(1)-N(6) = 71.58 (4), O(1)-Co(1)-N(6) =86.58(7), N(3)-Co(1)-N(6) = 147.94(8), N(1)-Co(1)-N(6) = 147.94(8)140.42(8).

Single-crystal X-ray analysis of Co2 revealed two crystallographically independent molecules per asymmetric unit. The cobalt center adopts a distorted octahedral geometry, coordinated equatorially by four nitrogen atoms from the dpzMe2phen ligand and axially by two water molecules. The phenanthroline nitrogen atoms form acute bite angles  $(N(1)-Co(1)-N(3) = 71.53^{\circ})$ , characteristic of phenanthroline chelation, (18) leading to elongation of the Co-N bonds (Co-N(3) = 2.100 Å, Co-N(4) = 2.095 Å) relative to the pyrazolyl-Co bonds (Co–N(1) = 2.215 Å, Co– N(6) = 2.217 Å). This bond length variation alleviates strain within the rigid tetradentate framework. Coordination strength differences are attributed to steric and electronic effects. Notably, the axial Co-O bonds differ slightly (O(1)-Co(1) = 2.100 Å vs. O(2) - Co(1) = 2.044 Å), and the O(2) -Co(1)–N(4) bond angle (104.26°) confirms a distortion from ideal octahedral geometry, influenced by ligand repulsion and electronic factors.

#### 3.2 Photocatalytic studies

The catalytic performance of cobalt (Co1-Co3) complexes was evaluated under identical reaction conditions, including 50.0  $\mu$ M catalyst, 0.3 mM [Ru(bipy)<sub>3</sub>]<sup>2+</sup> as a photosensitizer, and 0.11 M BIH as a sacrificial reductant in a CO<sub>2</sub>-saturated aqueous CH<sub>3</sub>CN solution (7.5 % v/v) at 308 K (Scheme 2).





Scheme 2. Structures of Co1-Co3, [Ru(bipy)<sub>3</sub>]<sup>2+</sup> and BIH.

The reactions were conducted under visible light irradiation ( $\lambda = 460$  nm) for 24 hours, unless otherwise specified. The data is presented in Table 1. The gas products (CO and H<sub>2</sub>) were quantified by headspace analysis with gas chromatography. A blank experiment without catalyst (entry 1) showed minimal activity, confirming the necessity of the cobalt complex for efficient CO<sub>2</sub> reduction. Among the three catalysts, Co2 emerged as the most efficient, delivering the highest CO production (TON<sub>CO</sub> = 896) and selectivity (82%) as compared to Co1 and Co3 (Figure 1).

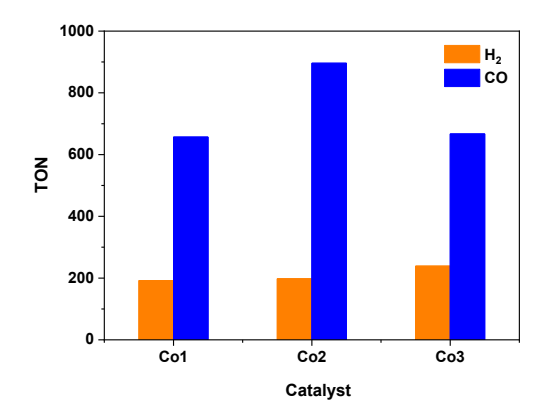


Figure 1. TON for photocatalytic CO<sub>2</sub>-to-CO conversion by Co<sub>1</sub>-Co<sub>3</sub> catalysts in aqueous CH<sub>3</sub>CN (7.5 % H<sub>2</sub>O).

The higher TON displayed by Co2 can be associated to the nature of the 3,5-substituents on the pyrazolyl ligand, which modulate the electronic properties of the cobalt center. Thus, the electron-donating methyl groups enhance the electron density at the cobalt center, facilitating reduction from Co(II) to Co(I) and stabilizing key intermediates involved in CO<sub>2</sub> activation. Conversely, Co1, which lacks substituents at the 3,5-positions, exhibits a lower TON<sub>CO</sub> of 657 and slightly reduced selectivity (77%). The absence of electron-donating groups renders the cobalt center less electron-rich, which can impair efficient CO2 activation and favor H2 evolution. Additionally, the smaller steric profile may increase the accessibility of the metal center to protons in solution, further contributing to reduced CO selectivity. Co3, bearing a phenyl group at the 3position of the pyrazolyl ring, also underperforms relative to



Co2, with a TON<sub>CO</sub> of 667 and selectivity of 74%. Here, both electronic and steric factors may be detrimental. The phenyl ring introduces significant bulk, potentially distorting the coordination geometry or hindering substrate access. Moreover, its mildly electron-withdrawing character (via inductive effects) could reduce the electron density at the metal center, similarly to Co1, but with added steric encumbrance. These combined effects may explain the increased tendency for proton reduction, as reflected in its higher TON<sub>H2</sub> (239). Similar results were found for the iron complexes bearing identical bis-(pyrazolyl)phenanthroline ligands.(15)

The impact of irradiation time on the photocatalytic performance of Co2 was systematically evaluated by comparing entries 3, 8–10 (Table 1). As presented in Figure 2, a clear trend was observed, where the TON<sub>CO</sub> increased with longer irradiation times, reaching 1136 after 72 h. However, the rate of increase diminished significantly after 24 h, suggesting a gradual approach to a kinetic or material limitation, potentially associated with partial catalyst deactivation, sacrificial donor (BIH) depletion, or accumulation of inhibitory by-products.

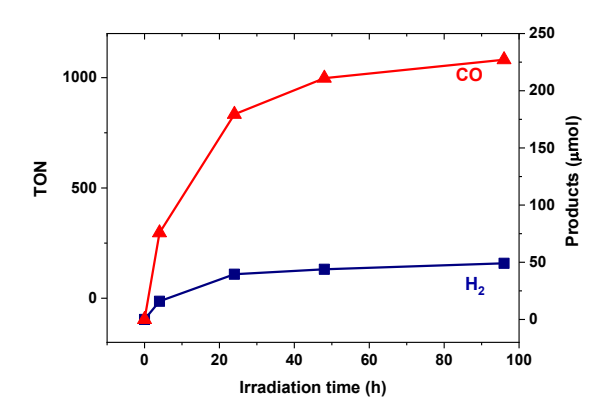


Figure 2. Evolution of the production of CO and  $H_2$  with the irradiation time using Co2.

In parallel, the  $TON_{H_2}$  also increased but to a lesser extent, with a notable plateauing behavior (75  $\rightarrow$  198  $\rightarrow$  219  $\rightarrow$  232 from 4 to 72 h), indicating that hydrogen evolution became increasingly suppressed relative to CO production over time. Significantly, the CO selectivity remained remarkably stable across all irradiation times, consistently around 82–83%, demonstrating that the intrinsic preference of Co2 for CO2 reduction over proton reduction was preserved even during prolonged operation. These results highlight the robustness of Co2 under continuous visible-light irradiation, maintaining high selectivity and substantial activity, while also underscoring the necessity of strategies such as sacrificial donor replenishment or catalyst regeneration to





further extend the productive lifetime of the system under extended irradiation conditions.

The influence of catalyst concentration on the photocatalytic reduction of CO<sub>2</sub> was also systematically

explored. The data is presented in Table 1 (entries 3 and 5–7) and displayed in Figure 3.

Table 1. Visible-light-drive catalytic reduction of CO<sub>2</sub> by cobalt complexes.<sup>a</sup>

|       |              | Conc. | Time | H <sub>2</sub> O | TON               |       | [H]    | [CO]   | Sel. CO |
|-------|--------------|-------|------|------------------|-------------------|-------|--------|--------|---------|
| Entry | Catalys<br>t | (μΜ)  | (h)  | (%)              | (H <sub>2</sub> ) | (CO)  | (µmol) | (µmol) | (%)*    |
| $1^b$ | -            | 0.00  | 24   | 7.5              | 14                | 61    | 16.8   | 73.2   | 81      |
| 2     | Co1          | 50.0  | 24   | 7.5              | 192               | 657   | 38.4   | 131.4  | 77      |
| 3     | Co2          | 50.0  | 24   | 7.5              | 198               | 896   | 39.6   | 179.4  | 82      |
| 4     | Co3          | 50.0  | 24   | 7.5              | 239               | 667   | 47.9   | 133.4  | 74      |
| 5     | Co2          | 25.0  | 24   | 7.5              | 689               | 1834  | 68.9   | 183.4  | 73      |
| 6     | Co2          | 12.5  | 24   | 7.5              | 311               | 5335  | 15.5   | 266.8  | 95      |
| 7     | Co2          | 6.25  | 24   | 7.5              | 764               | 11753 | 19.1   | 293.8  | 94      |
| 8     | Co2          | 50.0  | 4    | 7.5              | 75                | 362   | 15.9   | 75.8   | 83      |
| 9     | Co2          | 50.0  | 48   | 7.5              | 219               | 1055  | 43.9   | 211.0  | 83      |
| 10    | Co2          | 50.0  | 72   | 7.5              | 232               | 1136  | 49.1   | 227.1  | 82      |

a Reaction conditions unless specified otherwise: 50.0 μM catalyst, 0.3 mM [Ru(bipy)<sub>3</sub>]<sup>2+</sup> and 0.11 M BIH, 24 h in a CO<sub>2</sub>-saturated MeCN/H<sub>2</sub>O solution (4 mL) at 308 K upon visible light irradiation (460 nm). <sup>b</sup> Without catalyst. All experiments were performed at least two times, having good reproducibility (error 5–10%),\* Sel<sub>CO</sub> = [mmol(CO)/(mmol(H<sub>2</sub>)+mmol(CO)]x100.

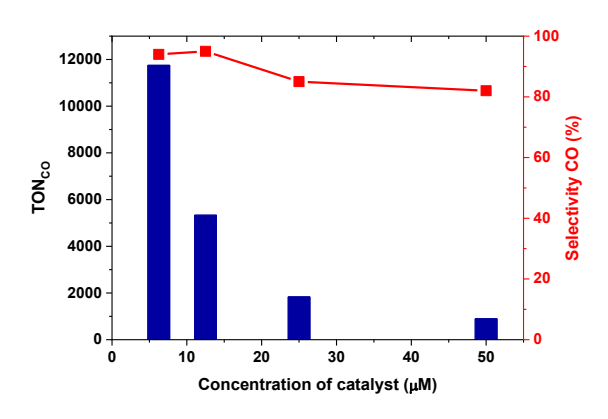


Figure 3. Concentration dependence of Co2 on  $TON_{CO}$  and selectivity.

A strong inverse correlation between catalyst concentration and  $TON_{CO}$  was observed: decreasing the concentration of Co2 from 50.0  $\mu M$  to 6.25  $\mu M$  resulted in a dramatic increase in  $TON_{CO}$  from 896 to 11.753. This trend

highlights that lower catalyst loadings significantly enhance catalytic efficiency, likely due to reduced aggregation, minimized self-quenching with the photosensitizer, and improved light penetration throughout the reaction medium. Notably, CO selectivity also improved markedly at lower concentrations, increasing from 82% at 50.0 µM to 94–95% at 6.25-12.5 µM, suggesting that proton reduction was suppressed and single-electron transfer processes leading to CO<sub>2</sub> reduction were favored under these conditions. While TON<sub>H2</sub> initially increased at intermediate concentrations (25.0 µM), a substantial decrease in hydrogen evolution was observed at lower catalyst loadings, further emphasizing the preferential formation of CO. Overall, these results demonstrate that optimizing catalyst concentration is critical for achieving high turnover and selectivity, revealing that dilution of Co2 enhances both the efficiency and specificity of the photocatalytic system under visible light irradiation.



# 4. Conclusion

We report the synthesis, characterization, photocatalytic evaluation of cobalt(II) bis(pyrazolyl)phenanthroline complexes (Co1-Co3) for the visible-light-driven reduction of CO<sub>2</sub> to CO. The complexes were fully characterized, and the structure of Co2 was confirmed by single-crystal X-ray diffraction, revealing a distorted octahedral geometry with four nitrogen donors from the dpzMe2phen ligand and two axial water molecules. Photocatalytic tests using  $[Ru(bipy)_3]^{2+}$  as photosensitizer and BIH as sacrificial donor showed that Co2, bearing electron-donating methyl groups, exhibited superior activity and selectivity ( $TON_{CO} = 896$ , 82% selectivity after 24 h) compared to Co1 and Co3. The enhanced performance of Co2 is attributed to electronic effects that facilitate Co(II)/Co(I) reduction and stabilize key intermediates. Systematic studies demonstrated that lowering catalyst concentration dramatically increases TON and CO selectivity, reaching  $TON_{CO} = 11753$  and 94-95%selectivity at 6.25-12.5 µM, likely due to reduced aggregation, minimized self-quenching, and improved light penetration. Extending irradiation time further increased CO production, although with reduced efficiency beyond 24 h, while maintaining high CO selectivity (82-83%). These results underscore the potential of electronically tailored cobalt(II) complexes as efficient and selective homogeneous photocatalysts for CO<sub>2</sub> valorization under mild conditions. Complementary investigations using Uv-vis spectroscopy, cyclic voltammetry and density functional theory (DFT) calculations are underway to further elucidate the mechanistic pathways involved.

# 5. Acknowledgments

The authors are gratefully acknowledged by RITE-FAPERGS (Grant/Award Number: 22/2551-0000386-9) and INCT/CNPq-Catálise (Grant/Award Number 465454/2014-3) for the financial support.

# 6. References

- 1. Nocera, D. G. Acc. Chem. Res. 2017, 50, 616-619.
- 2. Takeda, H.; Cometto, C.; Ishitani, O.; Robert, M. *ACS Catal.* **2017**, *7*, 70–88.
- 3. Pannwitz, A.; Klein, D. M.; Rodríguez-Jiménez, S.; Casadevall, C.; Song, H.; Reisner, E.; Hammarström, L.; Bonnet, S. *Chem. Soc. Rev.* **2021**, *50*, 4833–4855.
- 4. Appel, A. M.; Bercaw, J. E.; Bocarsly, A. B.; Dobbek, H.; DuBois, D. L.; Dupuis, M.; Fujita, E.; P. J. A.; Morris, R. H.; Peden, C. H. F.; Portis, A. R.; Ragsdale, S. W.; Rauchfuss, T. B.; Reek, J. N. H.; Seefeldt, L. C.; Thauer, R. K.; Waldrop, G. L. *Chem. Rev.* **2013**, *113*, 6621–6658.
- 5. Tang, B.; Xiao, F.-X. ACS Catal. 2022, 12, 9023-9057.



- 6. Kunene, T.; Xiong, L.; Rosenthal, J. Proc. *Natl. Acad. Sci. U. S. A.* **2019**, *116*, 9693–9695.
- 7. Rosenthal, J. *In Prog. Inorg. Chem.*, Karlin, K. D., Ed.; Wiley: Hoboken, NJ, **2014**, 59, 40.
- 8. Masdeu-Bultó, A. M.; Reguero, M.; Claver, C., *Eur. J. Inorg. Chem.* **2022**, e202100975.
- 9. Dalle, K. E.; Warnan, J.; Leung, J. J.; Reuillard, B.; Karmel, I. S.; Reisner, E. *Chem. Rev.* **2019**, *119*, 2752–2875.
- 10. Ma, F.; Luo, Z.-M.; Wang, J.-W.; Aramburu-Trŏselj, B. M.; Ouyang, G. *Coord. Chem. Rev.* **2024**, *500*, 215529.
- 11. Zhang, X.; Yamauchi, K.; Sakai, K. ACS Catal. **2021**, *11*, 10436–10449.
- 12. Boudreaux, C. M.; Nugegoda, D.; Yao, W.; Le, N.; Frey, N. C.; Li, Q.; Qu, F.; Zeller, M.; Webster, C. E.; Delcamp, J. H.; Papish, E. T., *ACS Catal.* **2022**, *12*, 8718–8728.
- 13. Ho, P.-Y.; Cheng, S.-C.; Yu, F.; Yeung, Y.- Y.; Ni, W.-X.; Ko, C.-C.; Leung, C. F.; Lau, T.-C.; Robert, M. *ACS Catal.* **2023**, *13*, 5979–5985.
- 14. Chapovetsky, A.; Welborn, M.; Luna, J. M.; Haiges, R.; Miller, T. F.; Marinescu, S. C. *ACS Cent. Sci.* **2018**, *4*, 397–404.
- 15. Zhu, M.; Ye, R.; Jin, K.; Lazouski, N.; Manthiram, K. *ACS Energy Lett.* **2018**, *3*, 1381–1386.
- 16. Sampaio, R. N.; Grills, D. C.; Polyansky, D. E.; Szalda, D. J.; Fujita, E. *J. Am. Chem. Soc.* **2020**, *142*, 2413–2428.
- 17. Ferreira Jr, J., Uez, G., Moro, A. V., Ludtke, D. S., Casagrande, A. C. A., Migowski, P., Rodembusch, F. S., Casagrande Jr, O. L. 23<sup>o</sup> Congresso Brasileiro de Catálise, 2025, Natal, RN, Brasil.
- 18. Potocnák, I.; Ráczová, K.; Cizmár, E.; Váhovská, L.; Bukrynov, O.; Vitushkina, S.; Findoráková, L., *Polyhedron* **2017**, *137*, 112–121.